

perpendicular to the substrate (within ca. 10°) for both of these monolayers.^{3,6} The third monolayer, perfluorinated acid ester (PFAE), was used to test the effect of lower surface energy and heavier chain constituents. This monolayer, also prepared by self-assembly on glass,⁶ is entirely fluorinated over the outer eight carbons of the chain, exposing the $-\text{CF}_3$ group. Freshly cleaved LiF(100) faces were used to estimate the time resolution of the experiment in the case of elastic scattering.

The TOF studies were made in a three-tiered vacuum chamber. From the nozzle expansion region, the pulsed molecular beam (R. M. Jordan Co., nominal 50- μs width) expands through a skimmer into the sample chamber where it is collimated and then strikes the surface of the sample, which is mounted on a rotatable mount. The quadrupole mass spectrometer (UTI model 100 C) is located 40 cm from the sample and differentially pumped. If it is positioned closer, sample degradation occurs. Overall angular resolution is 5° . The nozzle-sample-detector angle is fixed at 60° . The TOF trace, triggered from the firing of the pulse nozzle, is averaged by use of a PC-controlled digital scope (Gould) over 500–2000 shots. The scattered signal was easily discerned when superimposed on the rising peak of unpumped gas from each nozzle pulse. Appropriate background subtraction was made, and the TOF traces were analyzed only up to the point where the difference between directly scattered and background ion signals was significant.

A preliminary study was made of the angular scattering distribution. Whereas scattering of He from LiF yielded strong scattered signals with specular and diffraction peaks observable, the monolayers all gave a weak, diffuse pattern centered about the surface normal. Such patterns may be indicative of a dirty or rough surface, and so it is worthwhile to emphasize here some of the qualities of these monolayers. Because these surfaces are of low energy (< 20 dyn/cm compared with > 1000 dyn/cm for typical metal surfaces),^{7,8} we do not expect them to become contaminated even under the mild vacuum conditions (10^{-7} – 10^{-6} Torr) of this experiment. No change in contrast angles measured before and after the experiment could be observed. This indicated that neither contamination nor deterioration of the monolayer structure occurred.^{3,4,9} In addition, two recent publications have shown that similar surfaces remain clean, as measured by Auger spectroscopy⁹ and LEED.¹⁰ These surfaces, prepared in the former case by self-assembly and in the latter case by the Langmuir-Blodgett method, are by necessity prepared under atmospheric conditions and then transferred to vacuum for study without further cleaning. With respect to surface roughness, we have prepared the monolayers on the mica, silicon crystal, and LiF crystals in order to see if the surface smoothness would affect the scattering patterns. X-ray studies have shown that the roughness of OTS prepared on polished

Si wafers is of the order of tenths of angstroms.¹¹ Cleaved mica and LiF surfaces are atomically smooth. It is reasonable to assume that their smoothness is preserved upon coating with ordered monolayers. The fact that every substrate yielded the same diffuse scattering pattern indicates that scattering properties of these monolayers are substrate independent.

TOF data gave supporting evidence for the above results. The TOF patterns obtained at different angles were identical within the accuracy of the experiment. Therefore we may presume that there is no component which contributes to particular angles only. Measurements of the TOF patterns reported here were generally made at normal deflection angle, and incident angle of 60° .

Before data analysis, TOF traces were shortened to preclude the nozzle-surface distance (12 cm) and take into account the gas pulse width. The ion flight time and spreading effect of the ionization volume were small corrections which were made on the derived parameters. Because the equations chosen for the fitting^{12,13} were velocity flux equations, they were transposed to density and the time frame in order to match the experimental curve. Two phenomena are included in the expression. The first component describes a Maxwellian stream at the surface temperature for probes which have completely accommodated to the surface. The second component is a distribution with both width and mean speed free to vary. We designate this nonequibrated portion the stream component [second term in Eq. (1)]. The advantage of this equation is that it allows characterization of the part of the scattered curve which is not described by a Maxwellian stress at the surface temperature:

$$I = (B/t^2)\exp\{(-m/2k_B T)(L^2/t^2)\} + (A/t^2)\exp[-W(L/tv_s - 1)^2]. \quad (1)$$

Here I is the signal intensity, m the mass of the gas, k_B Boltzmann's constant, and T the surface temperature which was fixed at 300 K. For the stream component, the width factor is $W = \gamma M_a^2/2$, M_a being the aerodynamic Mach number and γ the heat-capacity ratio C_p/C_v , but we attach importance to W only as a measure of the width of the distribution (narrow for large W). The other quantities are stream velocity v_s , surface-detector distance L , and time t . A and B are the normalization constants for the stream and Boltzmann components, respectively.

In Fig. 2, TOF traces for He scattered from PFAE, LiF, and Cd(II) arachidate are displayed. The latter is similar to scattering from OTS on any of the substrates. Simulations obtained by fitting with Eq. (1) are overlaid on the experimental curves. From the curve fittings, best-fit values were obtained for W , v_s , A , and B . The fits were excellent, and unique with respect to parameter adjustment. In fact, the major source of uncertainty in the parameters is reproducibility between runs which

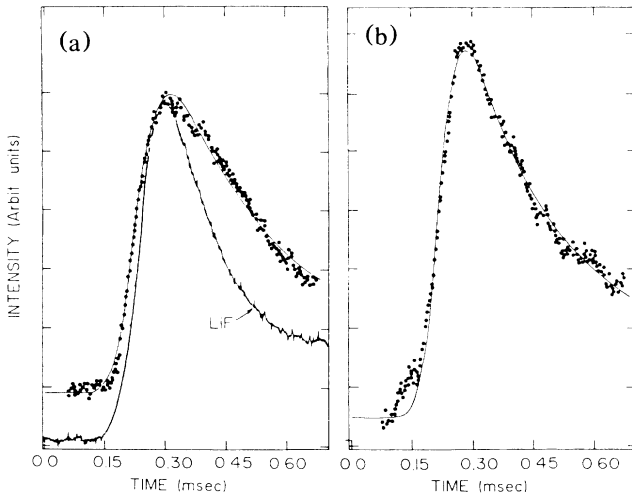


FIG. 2. Fitted TOF simulations (solid lines) overlaid on the experimental trace (dots) for He scattered from (a) OTS (with LiF curve underlaid for width comparison), and (b) PFAE.

averaged $\pm 8\%$ for v_s and $\pm 10\%$ for large W , approaching 100% for $W \approx 1$. Integration yielded the relative weights of the two components. In Table I the data are presented in two forms: On the left side the experimentally measured average energy loss and width of the distribution are displayed. On the right side the parameters obtained from the fitting are shown.

The data analysis was designed to give a both physically intuitive and simple representation of the results. It is important to note that for our unseeded beams, the incident kinetic energy is only very slightly larger than the most probable velocity of a Maxwellian stream leaving a room-temperature surface.¹³ This difference is larger for the diatomic gases. Exiting kinetic energy of the probe

therefore gives only partial information on the extent of energy transfer at the surface. For this reason, the width of the scattered distribution is an important measure of the extent of energy transfer because an increase of the width represents a loss of coherence between incoming and outgoing distributions. The kinetic-energy loss is probably dominated by partial migration into and tortuous exit from among the chains. This process may also contribute to coherence loss to a degree determined by the nature of probe and surface. This phenomenon will be expressed by a larger stream fraction with a low velocity v_s , in addition to possible diminution of W .

For He scattered from PFAE, it is clear that the stream portion is described by an exceptionally high width factor. In fact, W is almost identical to that obtained for He scattered from LiF (for LiF, the width factor was 11.6 with 70% stream). The kinetic-energy loss for this component is also quite low. This is indicative of a hard-impact, nearly elastic collision. It is interesting to contrast these data with those for He scattered from OTS, and Ar scattered from PFAE. The former gives a distribution which is essentially thermalized. The latter gives a width much smaller than the He case, but large enough to be considered nonthermalized. These differences may be understood by consideration of the mass ratio $\mu = (\text{gas mass})/(\text{surface mass})$ for the different cases. μ is small for He scattered from PFAE whether the surface unit is taken to be CF_3 or merely F. Energy transfer is poor because of the mismatch in masses. When the probe is the more massive Ar, the nearly even mass ratio allows significant energy transfer to occur. The OTS, besides being lighter, is also less rigid than the perfluorinated surface. Its behavior is more like a soft mattress than a hard wall.

The hard-cubes model¹⁴ was used to simulate the He-PFAE results. A good fitting was obtained if the total

TABLE I. Measured and fitted parameters for TOF Distribution.

Gas	Surface	Measured values		Percentage kinetic energy loss ^c ($\pm 10\%$)	Normalized ^d FWHM (± 0.1)	Fitted parameters		
		E_i^a (10^{-13} erg) ($\pm 5\%$)	E_f^b (10^{-13} erg) ($\pm 10\%$)			W^e	Percent stream ^f	v_s^e (cm/sec)
He	PFAE	1.0	0.72	28	0.38	10	23	1.6×10^5
	OTS	1.0	0.57	43	0.62	1.0	100	1.4×10^5
Ar	PFAE	1.0	0.96	4	0.48	5.0	25	5.5×10^4
	OTS	1.0	0.71	29	0.47	3.6	42	3.6×10^4
O ₂	PFAE	1.4	0.90	36	0.49	3	19	5.9×10^4
	OTS	1.4	0.80	43	0.49	2	53	5.2×10^4
NO	PFAE	1.5	0.68	54	0.43	2	63	5.2×10^4
	OTS	1.5	0.76	49	0.56	0.5	39	5.4×10^4

^aTranslational energy of incoming beam determined by fast ion gauge.

^bAverage translational energy of scattered distribution.

^c $(1 - E_f/E_i) \times 100$.

^dFull width at half maximum (FWHM) of scattered distribution di-

vided by its average velocity.

^eFrom Eq. (1).

^fIntegrated intensity for relative contribution of second component in Eq. (1), after conversion to flux distribution.

incident velocity was substituted for the incident normal velocity, and $\mu = 0.08$. This corresponds to a "surface mass" of about 50 u. Although the systems studied gave significant tangential momentum transfer which is not allowed in the hard-cubes model, our aim was to see if a meaningful value could be obtained for the surface mass. The correspondence attained lends support to the notion of an impulsive, angle-independent collision between the He and the CF₃ end group.

The results for the diatomic molecules lack information on internal energy disposal, and hence are not as easily understood. Oxygen, however, seems to follow trends similar to the monatomic gases. Separate experiments are under way to probe internal energy changes in NO scattered from these surfaces.

In summary, ordered monolayers of long-chain amphiphiles have been shown to demonstrate unique properties in the scattering of gaseous atoms and molecules. Whereas a high extent of thermalization always occurs, an indirectly scattered component is observed which appears to be dependent on μ and the monolayer rigidity. The diffuse scattering which is observed could be due to either structural or thermal effects. Whereas the methyl groups introduce a certain degree of roughness, monolayers prepared on atomically smooth surfaces do not show any specular component, even for diatomic molecules which should be less sensitive to this structure because of their size. For this reason we must consider the role of thermal scattering. Because significant tangential momentum transfer has occurred, the surface modes involved in the scattering must have a component perpendicular to the carbon skeleton. In terms of the three surface modes described earlier, the end-group rotation and concerted waving motion could lead to kinetic-energy transfer in this direction. A low-frequency beating mode of the coupled C-C oscillators could conceivably provide good energy matching with the incoming probe. However, this motion is directed perpendicular to the surface

and thus cannot explain the scattering observed. For PFAE, the CF₃ group seems to control the scattering.

We gratefully acknowledge the support of the U. S.-Israel Binational Foundation, and partial support by a grant from the European Research Office of the U. S. Army.

¹J. A. Barker and D. J. Auerbach, *Surf. Sci. Rep.* **4**, 59 (1983), and references therein.

²W. A. Steele, *The Interaction of Gases with Solid Surfaces* (Pergamon, London, 1980).

³R. Maoz and J. Sagiv, *J. Colloid Interface Sci.* **100**, 465 (1984); J. Gun, R. Iscovici, and J. Sagiv, *J. Colloid Interface Sci.* **101**, 201 (1984).

⁴L. Netzer, R. Iscovici, and J. Sagiv, *Thin Solid Films* **99**, 235 (1983).

⁵R. Maoz, L. Netzer, J. Gun, and J. Sagiv, in *Proceedings of the Meeting on New Technological Applications of Phospholipid Bilayers, Thin Films and Vesicles, Tenerife, Spain, 6-9 January, 1986*, Plenum (to be published).

⁶D. L. Allara and R. G. Nuzzo, *Langmuir* **1**, 52 (1985).

⁷A. W. Adamson, *Physical Chemistry of Surfaces* (Wiley, New York, 1976).

⁸G. A. Somorjai, *Chemistry in Two Dimensions: Surfaces* (Cornell Univ. Press, 1981), Chap. 1.

⁹S. Garoff, R. B. Hall, H. W. Deckman, and M. S. Alvarez, *Proc. Electro-chem. Soc.* **85-88**, 112 (1985).

¹⁰V. Vogel, C. Woll, *J. Chem. Phys.* **84**, 5200 (1986).

¹¹M. Pomerantz, A. Segmüller, L. Netzer, and J. Sagiv, *Thin Solid Films* **132**, 153 (1985).

¹²J. B. Anderson and J. B. Fern, *Phys. Fluids* **8**, 780 (1965), Eq. (27). Because we used a pulsed beam and did not select velocities with a chopper, a different power of t is used in the stream portion of Eq. (1).

¹³F. O. Goodman and H. Y. Wachman, *Dynamics of Gas-Surface Scattering* (Academic, New York, 1976), Chap. 2.

¹⁴R. M. Logan, in *Solid State Surface Science*, edited by M. Green (Dekker, New York, 1973), pp. 42-47.